H1prelim-19-041
ZEUS-prel-19-001

Preliminary Writeup, April 4, 2019

HERAPDF2.0Jets NNLO (prel.), the completion of the HERAPDF2.0 family

H1, ZEUS and NNLOJET Collaborations

Abstract

The HERAPDF2.0 family, introduced in 2015, is completed with fits HERAPDF2.0Jets NNLO (prel.) based on inclusive HERA data and selected jet production data. The result of a fit with the strong coupling constant, $\alpha_s(M_Z^2)$, free is $\alpha_s(M_Z^2) = 0.1150 \pm 0.0008(\text{exp})^{+0.0002}_{-0.0005}$ (model/parameterisation) ± 0.0006(hadronisation) $\pm$ 0.0027(scale). Sets of parton density functions, PDFs, from fits with fixed $\alpha_s(M_Z^2) = 0.115$ and $\alpha_s(M_Z^2) = 0.118$ are presented and compared. The PDFs from the fit with fixed $\alpha_s(M_Z^2) = 0.118$ are also compared to the PDFs from HERAPDF2.0 NNLO. Predictions from the PDFs of HERAPDF2.0Jets NNLO (prel.) with fixed $\alpha_s(M_Z^2) = 0.115$ are compared to the jet production data used as input. The predictions describe the data very well.

1 Introduction

Deep inelastic scattering (DIS) of electrons on protons, ep, at centre-of-mass energies of up to $\sqrt{s} \approx 320\,\text{GeV}$ at HERA has been central to the exploration of proton structure and quark–gluon dynamics as described by perturbative Quantum Chromo Dynamics (pQCD) [1].

The combination of H1 and ZEUS data on inclusive ep scattering and the subsequent pQCD analysis, introducing the family of parton density functions (PDFs) known as HERAPDF2.0, was a milestone for the exploitation[2] of the HERA data. The preliminary work presented here represents a completion of the HERAPDF2.0 family [2] with a fit at NNLO to HERA inclusive [2] and jet production data published separately by the ZEUS and H1 collaborations. This was not possible at the time of the original introduction of HERAPDF2.0 because a treatment at NNLO of jet production in ep scattering was not available then.

The name HERAPDF stands for a pQCD analysis within the DGLAP [3–7] formalism, where predictions from pQCD are fitted to data. These predictions are obtained by solving the DGLAP evolution equations at LO, NLO and NNLO in the $\overline{\text{MS}}$ scheme [8].

2 Procedure and Data

The inclusive and dijet production data [9–13], which were already used for HERAPDF2.0Jets NLO were again used for the analysis presented here. A new data set [14] published by the H1 collaboration on jet production in low Q^2 events, where Q^2 is the four-momentum-transfer squared, was added as input to the fits. All data sets on jet production, which were used, are listed in Table 1. The charm data, which were included in the analysis at NLO, were not used for the analysis presented here. Their influence will be studied in a future analysis.

The fits presented here were done in almost exactly the same way as for all other members of the HERAPDF2.0 family [2], and especially for the HERAPDF2.0Jets NLO fit. This includes the χ^2 definition which was taken from equation 32 of [2].

The fits were performed using the programme QCDNUM [15] within the xFitter, formerly HERAFitter, framework [16] and an independent programme, which was also already used as a second program in the HERAPDF2.0 analysis. The results obtained by the two programmes, as previously for all HERAPDF2.0 fits [2], were in excellent agreement, well within fit uncertainties. All numbers presented here were obtained using xFitter. Only cross sections for Q^2 starting at $Q^2_{min} = 3.5\,\text{GeV}^2$ were used in the analysis. All parameter setting were the same as for the HERAPDF2.0Jets NLO fit. The analysis of uncertainties was also performed in exactly the same way.

There were some modifications with respect to the analysis at NLO. They were driven by the usage of the newly available treatment of jet production at NNLO. The jet data were included in the fits at full NNLO using predictions for the jet cross sections calculated using NNLOJET [17–19], which was interfaced to the fast interpolation grid code, fastNLO [20–22] and APPLgrid [23,24] using the APPLfast framweork [25], in order to achieve the required speed for the convolution for use in an iterative PDF fit. As done previously, the predictions were multiplied by corrections for hadronisation and Z^0 exchange before they were used in the fits.

A running electro-magnetic α as implemented in the 2012 version of the programme EPRC [26] was used for the treatment of the jet cross sections.

The new treatment of inclusive jet and dijet production at NNLO was only applicable to a slightly reduced phase space compared to HERAPDF2.0Jets NLO. All data points with $\sqrt{\langle p_T^2 \rangle + Q^2} \leq 13.5\,\text{GeV}$ were excluded, where p_T is the transverse energy of the jets. In addition, six data points, the lowest $\langle p_T \rangle$ bin for each Q^2 region, were excluded from the ZEUS dijet data set because the NNLO predictions for these points were deemed unreliable. The resulting reduction of data points is listed in Table 1. In addition, the trijet data [13] which were used as input to HERAPDF2.0Jets NLO had to be excluded as their treatment at NNLO was not available.

The choice of scales was also adjusted to the NNLO analysis. At NLO, the factorisation scale was chosen as $\mu_\text{f}^2 = Q^2$, while the renormalisation scale was linked to the transverse momenta, p_T, of the jets by $\mu_\text{r}^2 = (Q^2 + p_T^2)/2$. For the NNLO analysis, $\mu_\text{f}^2 = \mu_\text{r}^2 = Q^2 + p_T^2$ was chosen.

3 Determination of the strong coupling constant

Jet production data are essential for the determination of the strong coupling constant, $\alpha_s(M_Z^2)$. In pQCD fits to inclusive DIS data alone, the gluon PDF is determined via the DGLAP equations only, using the observed scaling violations. This results in a strong correlation between the shape of the gluon distribution and the value of $\alpha_s(M_Z^2)$. Data on jet production cross sections provide an independent constraint on the gluon distribution. Jet and dijet production are also directly sensitive to $\alpha_s(M_Z^2)$ and thus such data allow for an accurate simultaneous determination of $\alpha_s(M_Z^2)$ and the gluon distribution.

The HERAPDF2.0Jets NNLO (prel.) fit with free $\alpha_s(M_Z^2)$ gave a value of

$$\begin{aligned}\alpha_s(M_Z^2) = 0.1150 \pm 0.0008(\text{exp})^{+0.0002}_{-0.0005}(\text{model/parameterisation}) \\ \pm 0.0006(\text{hadronisation}) \quad \pm 0.0027(\text{scale}) \quad .\end{aligned}$$

This result on $\alpha_s(M_Z^2)$ is compatible with the world average [27] and it is competitive to other determinations at NNLO. The "exp" denotes the experimental uncertainty which is taken as the fit uncertainty.

The HERAPDF2.0Jets NNLO (prel.) fit with free $\alpha_s(M_Z^2)$ uses 1343 data points and has a $\chi^2/\text{d.o.f.} = 1599/1328 = 1.203$. This can be compared to the $\chi^2/\text{d.o.f.} = 1363/1131 = 1.205$ for HERAPDF2.0 NNLO based on inclusive data only [2]. The similarity of the $\chi^2/\text{d.o.f.}$ values indicates that the data on jet production do not introduce any tension.

The experimental uncertainty was determined from the fit. The χ^2 scan in $\alpha_s(M_Z^2)$ shown in Fig. 1a) confirmed the value of $\alpha_s(M_Z^2)$ and the experimental, i.e. fit, uncertainty. The clear minimum coincides with the value as determined by the fit and the dependence of χ^2 on $\alpha_s(M_Z^2)$ confirms the fit uncertainty. The model/parameterisation and hadronisation uncertainties also shown in Fig. 1a) were determined with similar scans in the respective parameter spaces.

A strong motivation to determine $\alpha_s(M_Z^2)$ at NNLO was the hope to substantially reduce scale uncertainties. This uncertainty was evaluated by varying the renormalisation and factorisation scales by a factor of two, both separately and simultaneously, and taking the maximal positive and negative deviations. The uncertainties were assumed to be 50 % correlated and 50 % uncorrelated between bins and data sets. The result is also shown in Fig. 1a). The scale uncertainty still dominates the uncertainties.

As the input data were changed for the NNLO analysis and the choice of scales were changed with respect to the NLO analysis, a detailed comparison of scale uncertainties will be published after the appropriate reanalysis of the data at NLO. However, the scale uncertainty of ± 0.0027 is significantly lower than the $+0.0037, -0.0030$ previously observed for the HERAPDF2.0Jets NLO analysis. If the NNLO determination of $\alpha_s(M_Z^2)$ was performed with the old choice of scales, the value of $\alpha_s(M_Z^2)$ was reduced to 0.1135. This is well within scale uncertainties.

The question whether data with relatively low Q^2 bias the determination of $\alpha_s(M_Z^2)$ arose within the context of the HERAPDF2.0 analysis [2]. Figure 1b) shows scans with Q^2_{min} set to 3.5 GeV^2, 10 GeV^2 and 20 GeV^2 for the inclusive data. Clear minima are visible which coincide within uncertainties.

4 The PDFs of HERAPDF2.0Jets NNLO (prel.)

The PDFs resulting from the HERAPDF2.0Jets NNLO (prel.) fit with fixed $\alpha_s(M_Z^2) = 0.115$ are shown in Fig. 2 at a scale of $Q^2 = 10\,\text{GeV}^2$. The results of a full analysis of uncertainties obtained from the respective fits are also shown. This includes experimental, i.e. fit, uncertainties, model and parameterisation uncertainties as well as additional hadronisation uncertainties on the jet data, all as defined for the HERAPDF2.0 family [2].

The PDFs resulting from the HERAPDF2.0Jets NNLO (prel.) fit with fixed $\alpha_s(M_Z^2) = 0.118$, the value used for HERAPDF2.0Jets NLO, are shown in Fig. 3 at a scale of $Q^2 = 10\,\text{GeV}^2$. Also shown are the results of a full analysis of uncertainties. A comparison between the PDFs obtained for $\alpha_s(M_Z^2) = 0.115$ and $\alpha_s(M_Z^2) = 0.118$ is provided in Figs. 4 and 5 for the scale $10\,\text{GeV}^2$ and M_Z^2, respectively. Here, only total uncertainties are shown. At the lower scale, a significant difference is observed in the gluon distributions, where the distribution for $\alpha_s(M_Z^2) = 0.115$ is above the distribution for $\alpha_s(M_Z^2) = 0.115$ for x less than $\approx 10^{-2}$.

A comparison between the PDFs obtained by HERAPDF2.0Jets NNLO (prel.) with $\alpha_s(M_Z^2) = 0.118$ and the PDFs of HERAPDF2.0 NNLO based on inclusive data only is provided in Fig. 6. Again, only total uncertainties are shown. These two sets of PDFs do not show any significant difference.

5 Comparison of HERAPDF2.0Jets NNLO (prel.) to jet data

Comparisons of the predictions of HERAPDF2.0Jets NNLO (prel.) with fixed $\alpha_s(M_Z^2) = 0.115$ to the data on jet production used as input to the fits are shown in Figs. 7, 8, 9 and 10. The

H1 collaboration published most of their jet cross sections normalised to the inclusive NC cross sections.

All analyses were performed using the assumption of massless jets, i.e. the transverse energy, E_T, and the transverse momentum of a jet, p_T, are equivalent. For inclusive jet analyses, each jet is entered separately with its p_T. For dijet analyses, the average of the transverse momenta, $\langle p_T \rangle$ is used. In these cases, $\langle p_T \rangle$ was also used to set the the factorisation and renormalisation scales to $\mu_f^2 = \mu_r^2 = Q^2 + \langle p_T \rangle^2$ for calculating predictions. Scale uncertainties were not considered for the comparisons to data.

The predictions from HERAPDF2.0Jets NNLO (prel.) agree very well with all data on jet production used as input to the fit.

6 Summary

The HERA data set on inclusive ep scattering as introduced by the ZEUS and H1 collaborations [2], together with selected data on jet production, published separately by the two collaborations, were used as input to NNLO fits called HERAPDF2.0Jets NNLO (prel.). They complete the HERAPDF2.0 family. A fit with free $\alpha_s(M_Z^2)$ gave $\alpha_s(M_Z^2) = 0.1150 \pm 0.0008(\text{exp})^{+0.0002}_{-0.0005}(\text{model/parameterisation}) \pm 0.0006(\text{hadronisation}) \pm 0.0027(\text{scale})$. A preliminary set of PDFs with a full analysis of uncertainties was obtained from a HERAPDF2.0Jets NNLO (prel.) fit with fixed $\alpha_s(M_Z^2) = 0.115$. These PDFs were compared to PDFs from a similar fit with fixed $\alpha_s(M_Z^2) = 0.118$ and the PDFs from HERAPDF2.0 NNLO based on inclusive data only. All these PDFs are very similar. The predictions from HERAPDF2.0Jets NNLO (prel.) were compared to the jet production data used as input. The predictions describe the data very well.

7 Acknowledgements

We are grateful to the HERA machine group whose outstanding efforts have made the ZEUS and H1 experiments possible. We appreciate the contributions to the construction, maintenance and operation of the H1 and ZEUS detectors of many people who are not listed as authors. We thank our funding agencies for financial support, the DESY technical staff for continuous assistance and the DESY directorate for their support and for the hospitality they extended to the non-DESY members of the collaborations. We would like to give credit to all partners contributing to the EGI computing infrastructure for their support. We acknowledge the support of the IPPP Associateship program for this project.

References

[1] A. Cooper-Sarkar and R. Devenish, *Deep inelastic Scattering*, Oxford Univ. Press (2011), ISBN 978-0-19-960225-4.

[2] H. Abramovicz *et al.* [ZEUS and H1 Collaboration], Eur. Phys. J. C **75**, 580 (2015), [arXiv:1506.06042].

[3] V. N. Gribov and L. N. Lipatov, Sov. J. Nucl. Phys. **15**, 438 (1972).

[4] V. N. Gribov and L. N. Lipatov, Sov. J. Nucl. Phys. **15**, 675 (1972).

[5] L. N. Lipatov, Sov. J. Nucl. Phys. **20**, 94 (1975).

[6] Y. L. Dokshitzer, Sov. Phys. JETP **46**, 641 (1977).

[7] G. Altarelli and G. Parisi, Nucl. Phys. B **126**, 298 (1977).

[8] B. Fanchiotti, S. Kniehl and A. Sirlin, Phys. Rev. D **48**, 307 (1993), [hep-ph/9803393].

[9] S. Chekanov *et al.* [ZEUS Collaboration], Phys. Lett. B **547**, 164 (2002), [hep-ex/0208037].

[10] H. Abramowicz *et al.* [ZEUS Collaboration], Eur. Phys. J. C **70**, 965 (2010), [arXiv:1010.6167].

[11] A. Aktas *et al.* [H1 Collaboration], Phys. Lett. B **653**, 134 (2007), [arXiv:0706.3722].

[12] F. Aaron *et al.* [H1 Collaboration], Eur. Phys. J. C **67**, 1 (2010), [arXiv:0911.5678].

[13] V. Andreev *et al.* [H1 Collaboration], Eur. Phys. J. C **65**, 2 (2015), [arXiv:1406.4709].

[14] V. Andreev *et al.* [H1 Collaboration], Eur. Phys. J. C **77**, 215 (2017), [arXiv:1611.03421].

[15] M. Botje, Comp. Phys. Comm. **182**, 490 (2011), [arXiv:1005.1481].

[16] S. Alekhin *et al.* (2014), [arXiv:1410.4412].

[17] J. Currie, T. Gehrmann, and J. Niehues, Phys. Rev. Lett. **117**, 042001 (2016), [arXiv:1606.03991].

[18] J. Currie, T. Gehrmann, A. Huss, and J. Niehues, JHEP **1707**, 018 (2017), [arXiv:1703.05977].

[19] T. Gehrmann *et al.*, in *The Proceedings of the 13th International Symposium on Radiative Corrections (RADCOR2017), St.Gilgen, Austria* (2017), vol. 1707, [arXiv:1801.06415].

[20] T. Kluge, K. Rabbertz, and M. Wobisch (2006), [arXiv:1801.06415].

[21] T. Gehrmann *et al.*, in *20th International Workshop on Deep-Inelastic Scattering and Related Subjects (DIS 2012): Bonn, Germany* (2012), p. 217, [arXiv:1208.3641].

[22] D. Britzger *et al.*, *at DIS 2014* (2014), URL http://indico.cern.ch/event/258017/session/1/contribution/202.

[23] T. Carli, G. Salam, and F. Siegert (2005), [arXiv:0510324].

[24] T. Carli *et al.*, Eur. Phys. J. C **66**, 503 (2010), [arXiv:0911.2985].

[25] H. Collaboration [H1 Collaboration], Eur. Phys. J. C **77**, 791 (2017).

[26] H. Spiesberger, in *Proc. of Future Physics at HERA*, edited by G. Ingelman, A. De Roeck and R. Klanner (1995), p. 227.

[27] M. Tanabashi *et al.* (Particle Data Group), Phys. Rev. D **98**, 030001 (2018).

Data Set	taken		Q^2[GeV^2] range		$\mathcal{L}$	e^+/e^-	$\sqrt{s}$	norma-	all	used	Ref.
	from	to	from	to	pb^{-1}		GeV	lised	points	points	
H1 HERA I normalised jets	1999 – 2000		150	15000	65.4	e^+p	319	yes	24	24	[11]
H1 HERA I jets at low Q^2	1999 – 2000		5	100	43.5	e^+p	319	no	28	16	[12]
H1 normalised inclusive jets at high Q^2	2003 – 2007		150	15000	351	e^+p/e^-p	319	yes	30	24	[13], [14]
H1 normalised dijets at high Q^2	2003 – 2007		150	15000	351	e^+p/e^-p	319	yes	24	24	[13]
H1 normalised inclusive jets at low Q^2	2005 – 2007		5.5	80	290	e^+p/e^-p	319	yes	48	32	[14]
H1 normalised dijets at low Q^2	2005 – 2007		5.5	80	290	e^+p/e^-p	319	yes	48	32	[14]
ZEUS inclusive jets	1996 – 1997		125	10000	38.6	e^+p	301	no	30	30	[9]
ZEUS dijets 1998 –2000 &	2004 – 2007		125	20000	374	e^+p/e^-p	318	no	22	16	[10]

Table 1: The data sets on jet production from H1 and ZEUS used for the HERAPDF2.0Jets NNLO (prel.) fits.

a)

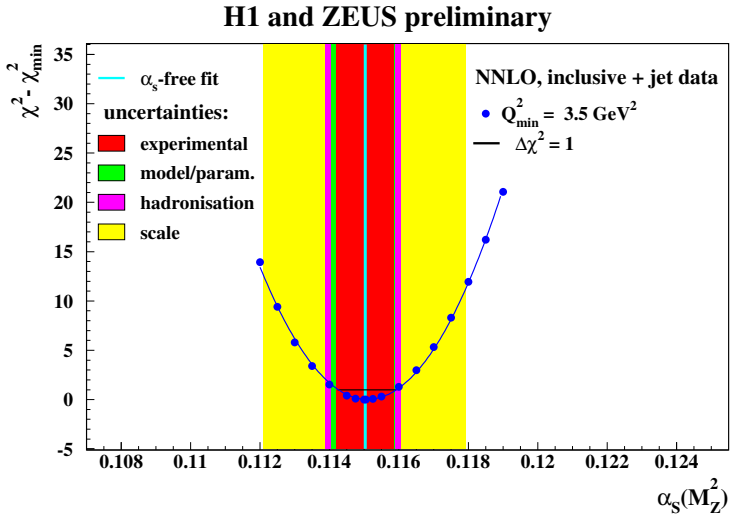

b)

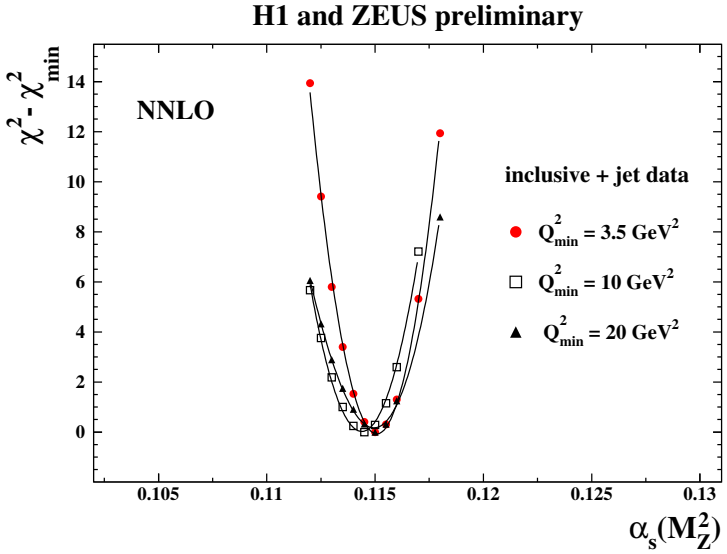

Figure 1: $\Delta\chi^2 = \chi^2 - \chi^2_{\text{min}}$ vs. $\alpha_s(M_Z^2)$ for HERAPDF2.0Jets NNLO (prel.) fits with fixed $\alpha_s(M_Z^2)$ with a) the standard Q^2_{min} of 3.5 GeV^2 b) with Q^2_{min} set to 3.5 GeV^2, 10 GeV^2 and 20 GeV^2 for the inclusive data. In a), the result and all uncertainties determined for the HERAPDF2.0Jets NNLO (prel.) fit with free $\alpha_s(M_Z^2)$ are also shown. In b), not all scan points for Q^2_{min} of 3.5 GeV^2 are plotted for better visibility.

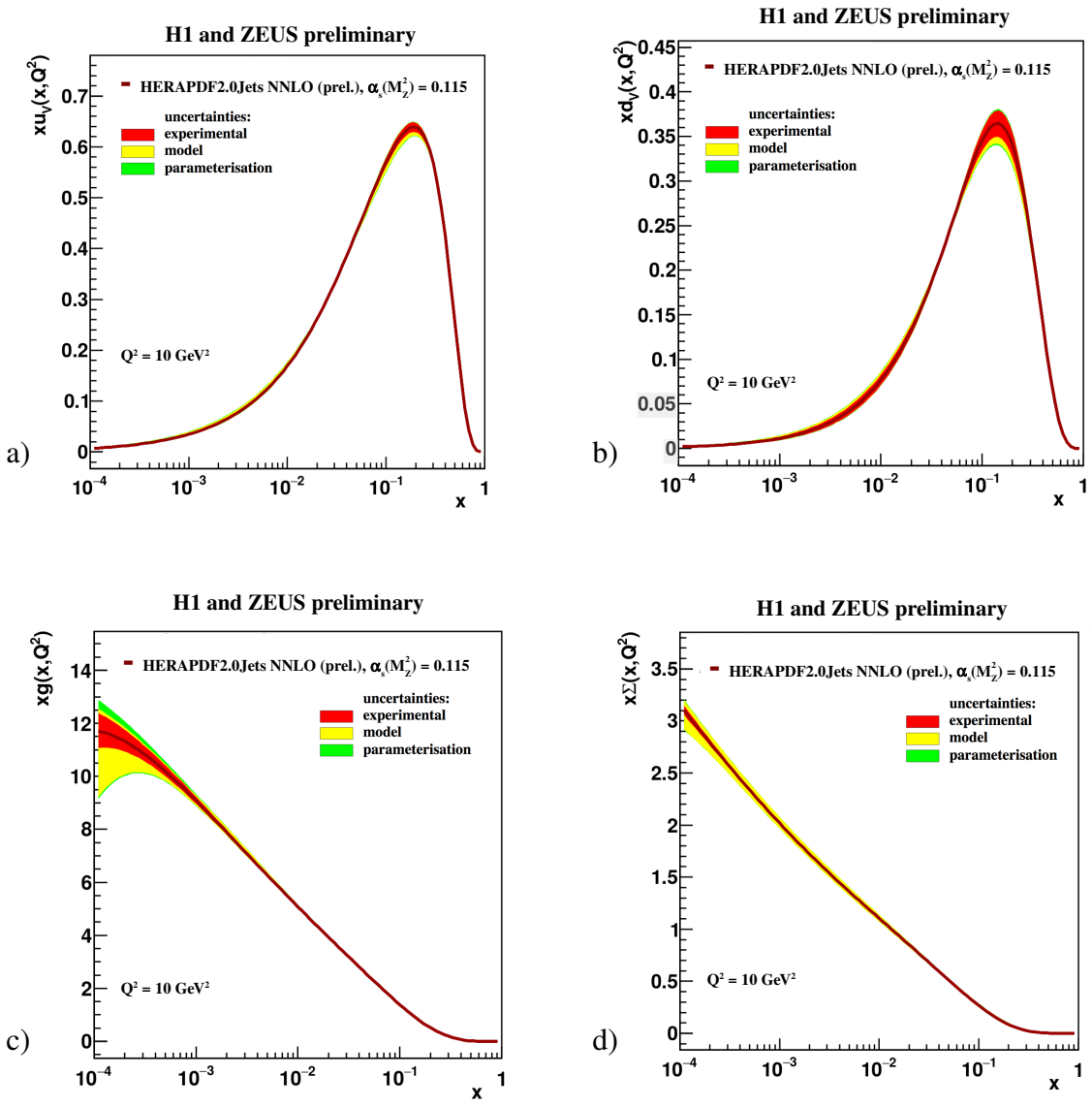

Figure 2: The parton distribution functions a) xu_v, b) xd_v, c) xg and d) $x\Sigma = x(\bar{U} + \bar{D})$ of HERAPDF2.0Jets NNLO (prel.) with $\alpha_s(M_Z^2)$ fixed to 0.115, the value determined in the NNLO fit with free $\alpha_s(M_Z^2)$ at the scale $Q^2 = 10\,\mathrm{GeV}^2$. The uncertainties are given as differently shaded bands.

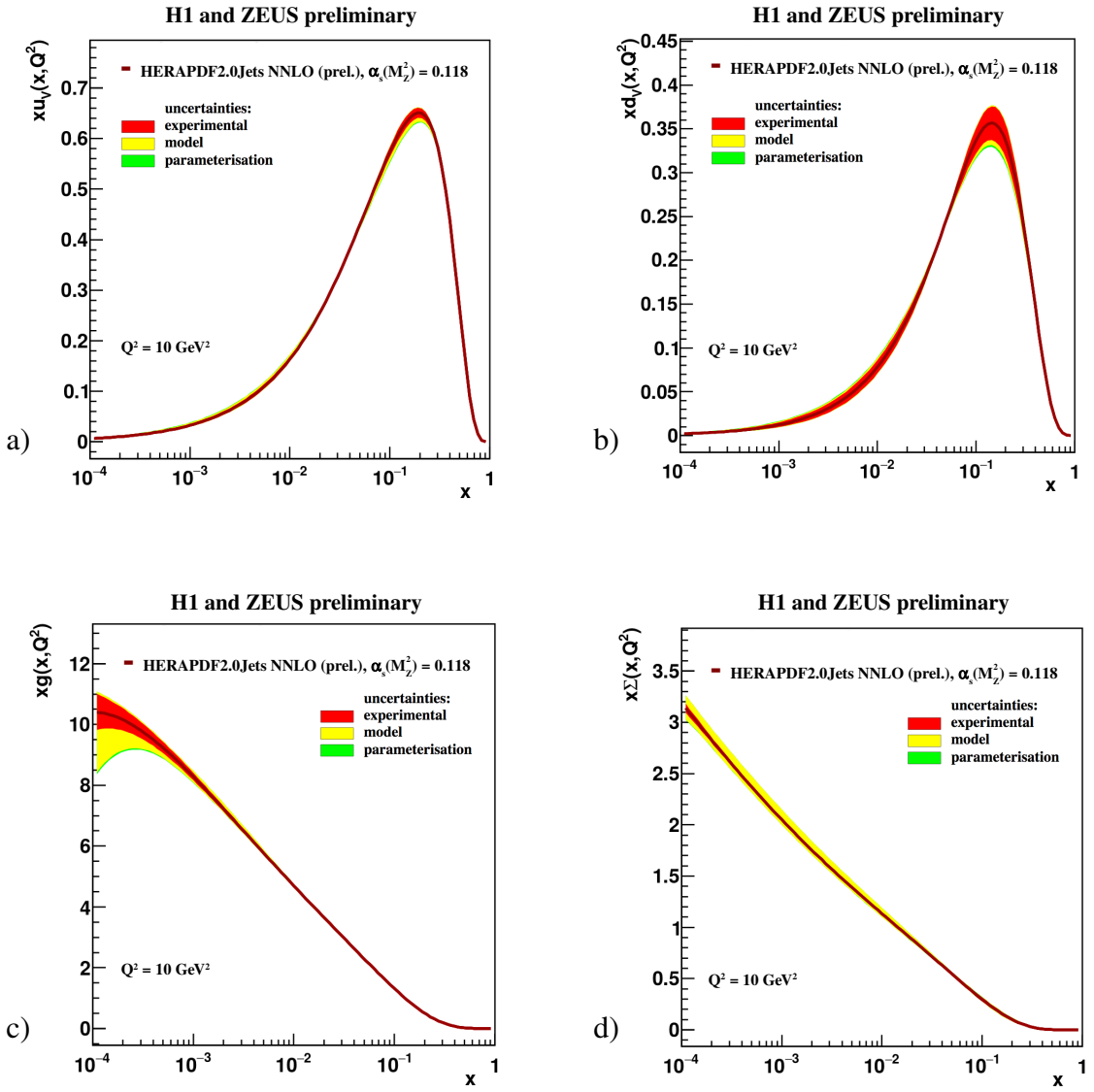

Figure 3: The parton distribution functions xu_v, xd_v, xg and $x\Sigma = x(\bar{U}+\bar{D})$ of HERAPDF2.0Jets NNLO (prel.) with $\alpha_s(M_Z^2)$ fixed to 0.118, the value determined in the HERAPDFJets NLO fit with free $\alpha_s(M_Z^2)$, at the scale $Q^2 = 10\,\mathrm{GeV}^2$. The uncertainties are given as differently shaded bands.

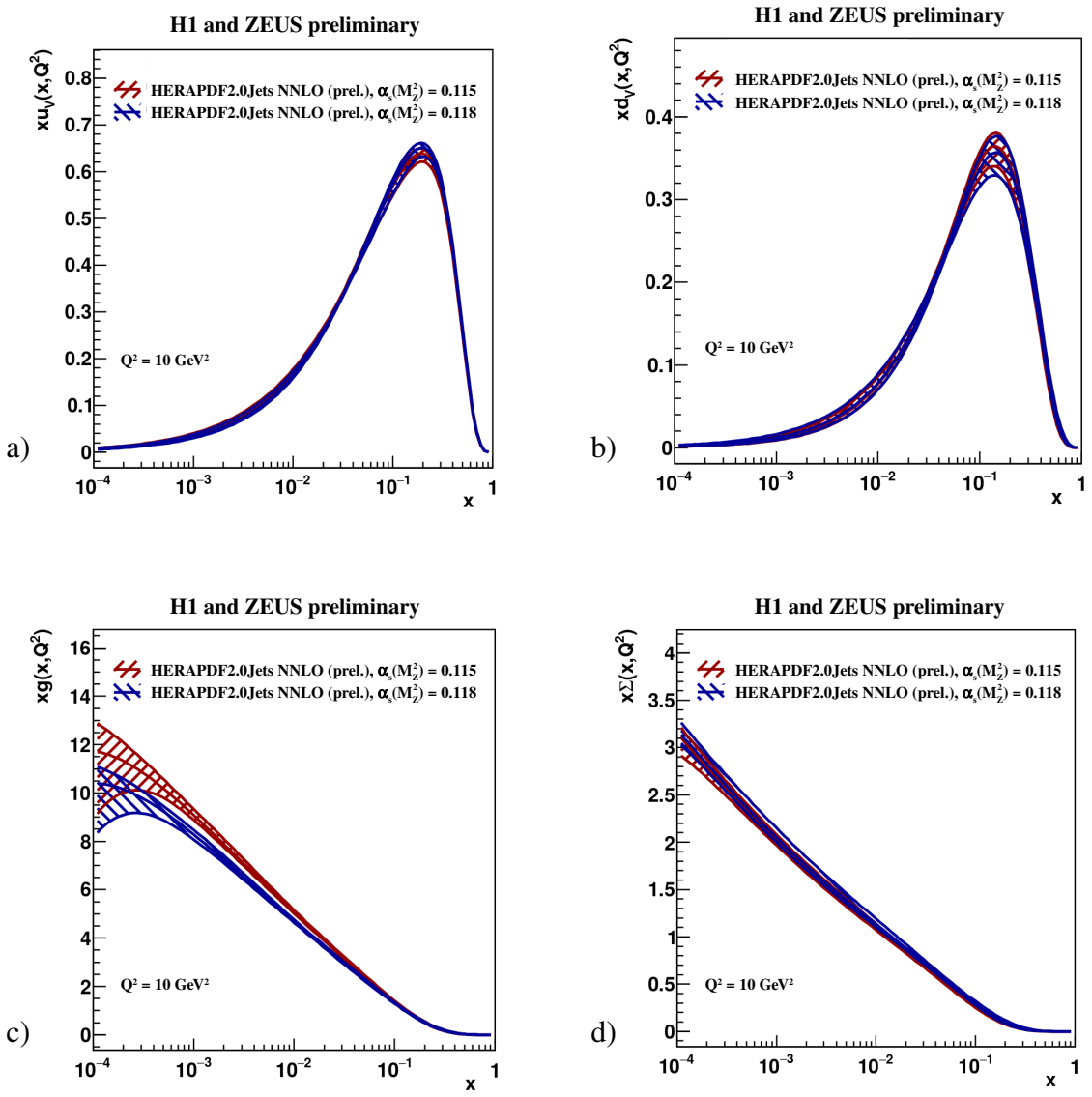

Figure 4: Comparison of the parton distribution functions a) xu_v, b) xd_v, c) xg and d) $x\Sigma = x(\bar{U} + \bar{D})$ of HERAPDF2.0Jets NNLO (prel.) with fixed $\alpha_s(M_Z^2) = 0.115$ and $\alpha_s(M_Z^2) = 0.118$ at the scale $Q^2 = 10\,\mathrm{GeV}^2$. The total uncertainties are shown as differently hatched bands.

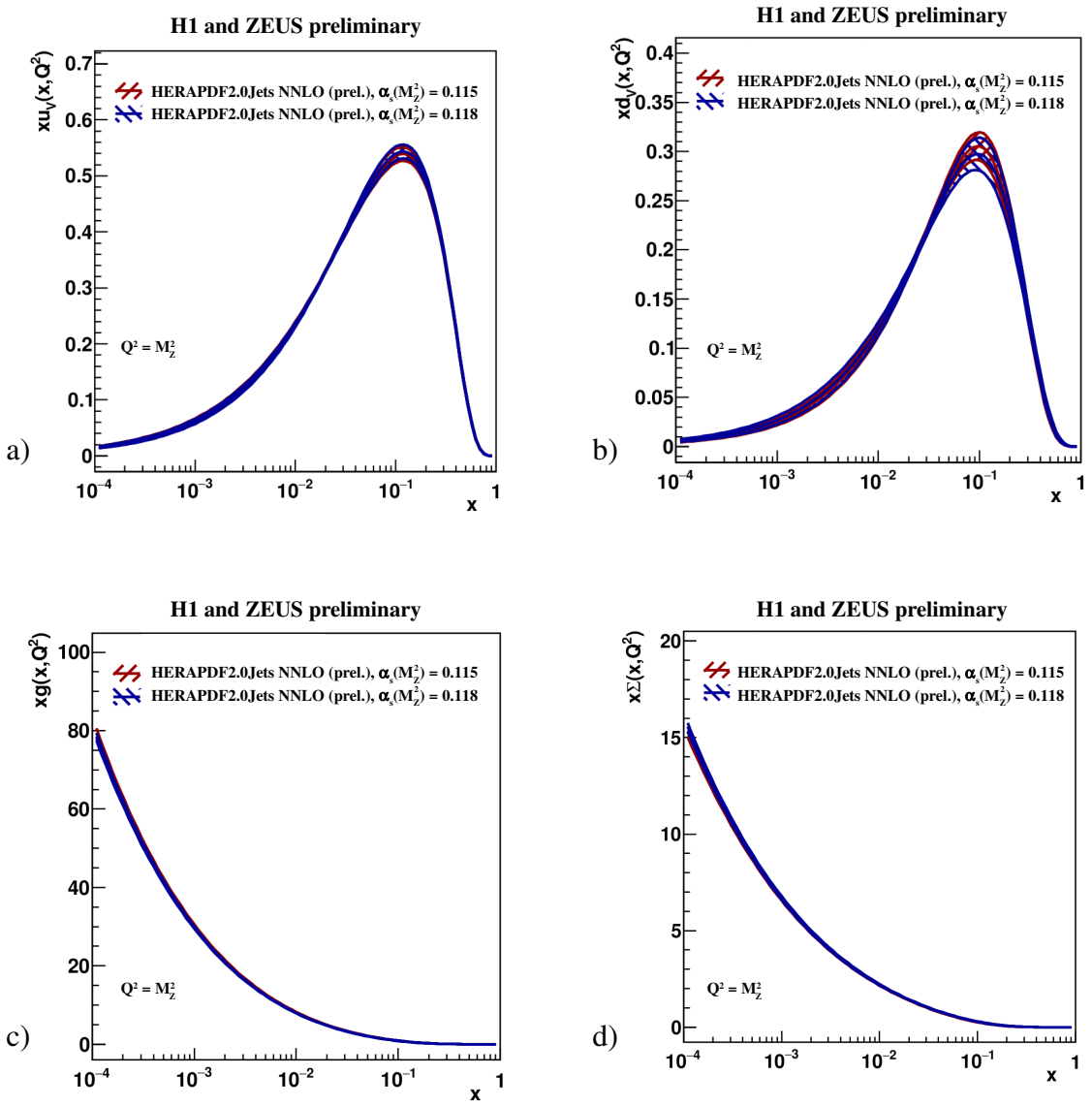

Figure 5: Comparison of the parton distribution functions a) xu_v, b) xd_v, c) xg and d) $x\Sigma = x(\bar{U} + \bar{D})$ of HERAPDF2.0Jets NNLO (prel.) with fixed $\alpha_s(M_Z^2) = 0.115$ and $\alpha_s(M_Z^2) = 0.118$ at the scale $Q^2 = M_Z^2$. The total uncertainties are shown as differently hatched bands.

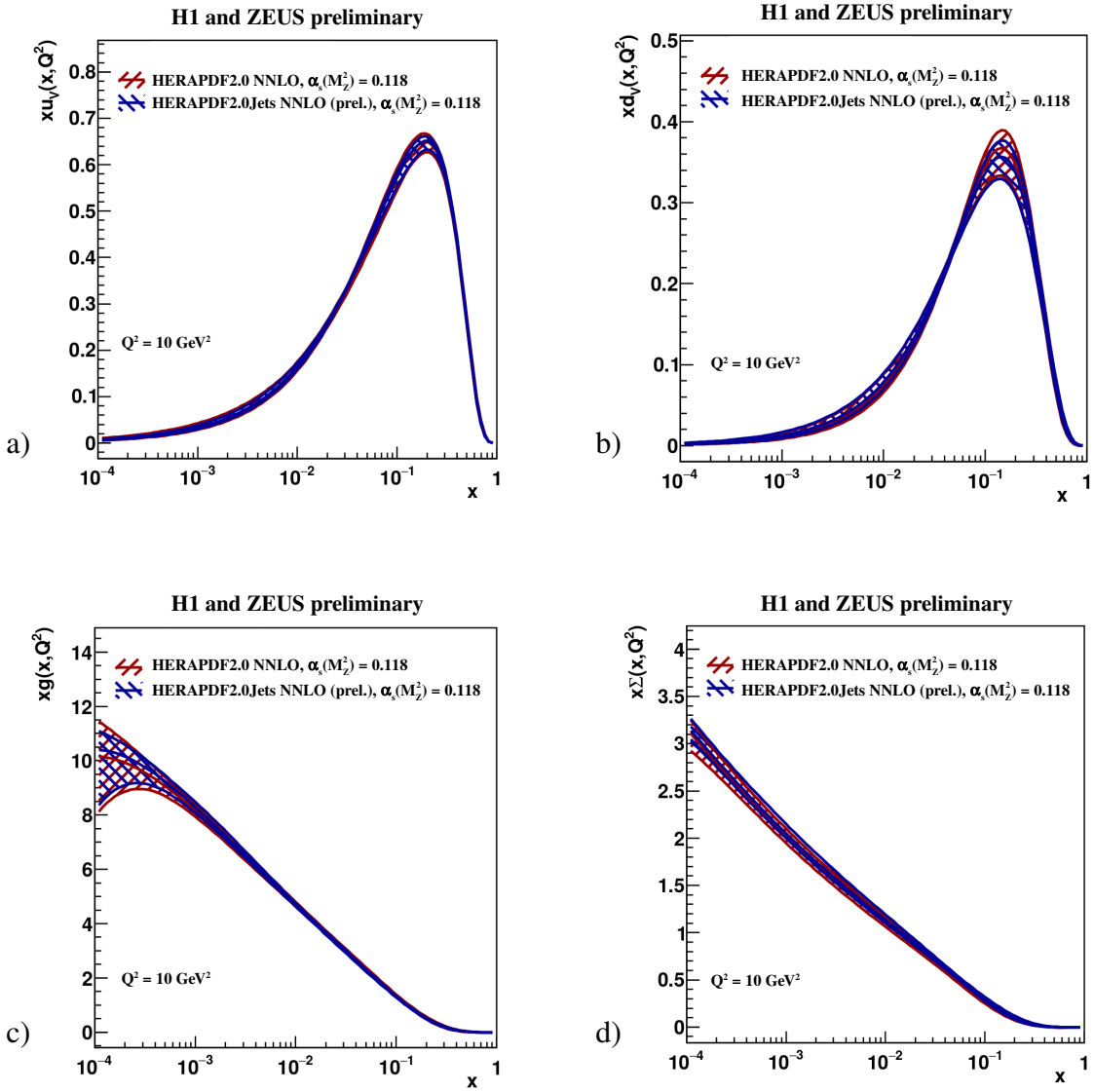

Figure 6: Comparison of the parton distribution functions a) xu_v, b) xd_v, c) xg and d) $x\Sigma = x(\bar{U} + \bar{D})$ of HERAPDF2.0Jets NNLO (prel.) and HERAPDF2.0 NNLO based on inclusive data only, both with fixed $\alpha_s(M_Z^2) = 0.118$, at the scale $Q^2 = 10\,\mathrm{GeV}^2$. The total uncertainties are shown as differently hatched bands.

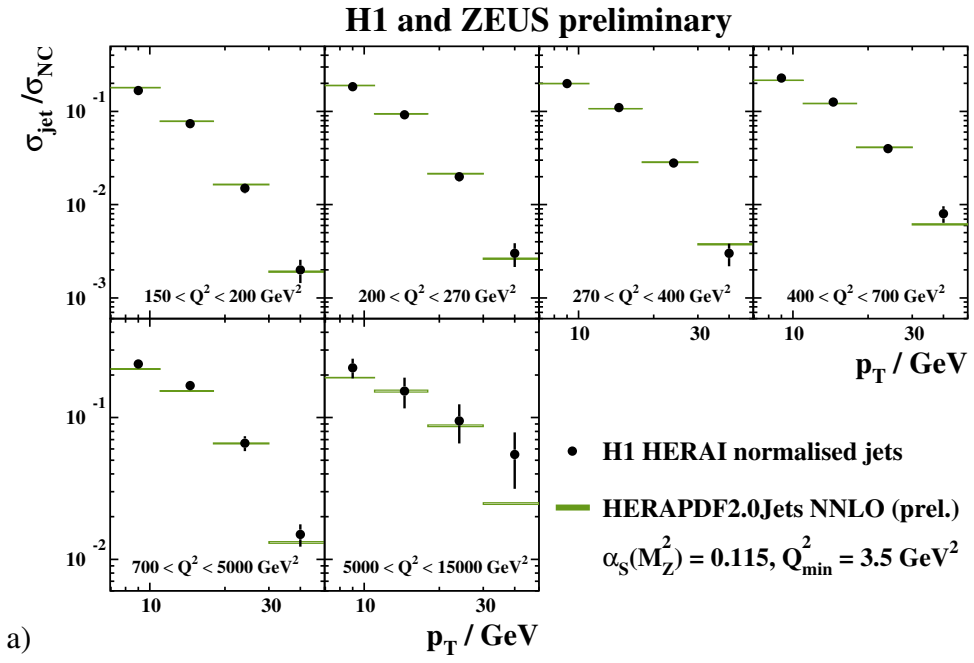

a)

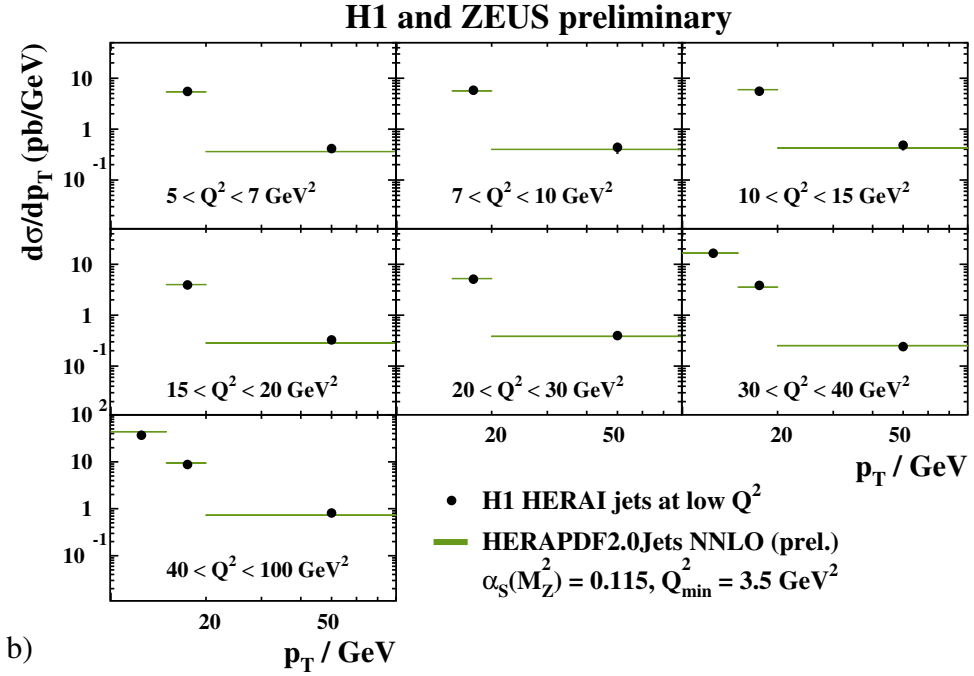

b)

Figure 7: a) Differential jet cross sections, $d\sigma/dp_T$, normalised to NC inclusive cross sections, in bins of Q^2 between 150 and 15000 GeV^2 as measured by H1. b) Differential jet cross sections, $d\sigma/dp_T$, in bins of Q^2 between 5 and 100 GeV^2 as measured by H1. Also shown are predictions from HERAPDF2.0Jets NNLO (prel.). The bands represent the total uncertainties on the predictions excluding scale uncertainties. Only data used in the fit are shown.

a)

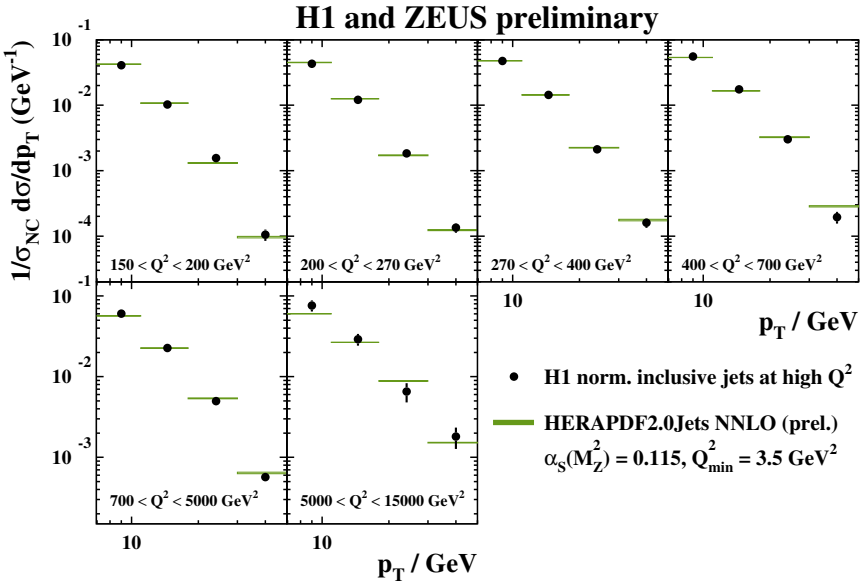

b)

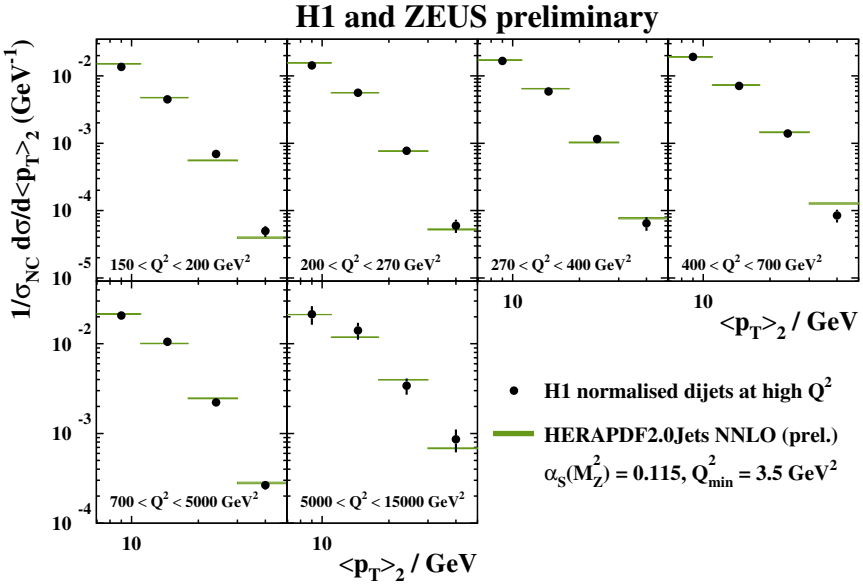

Figure 8: Differential normalised a) inclusive jet cross sections, $d\sigma/dp_T$, b) differential dijet cross-sections, $d\sigma/d\langle p_T\rangle_2$, in bins of Q^2 between 150 and 15000 GeV^2 as measured by H1. The variable $\langle p_T\rangle_2$ denote the average p_T of the two jets. All cross sections are normalised to NC inclusive cross sections and devided by the bin-width. Also shown are predictions from HERAPDF2.0Jets NNLO (prel.). The bands represent the total uncertainties on the predictions excluding scale uncertainties; they are mostly invisible. Only data used in the fit are shown.

a)

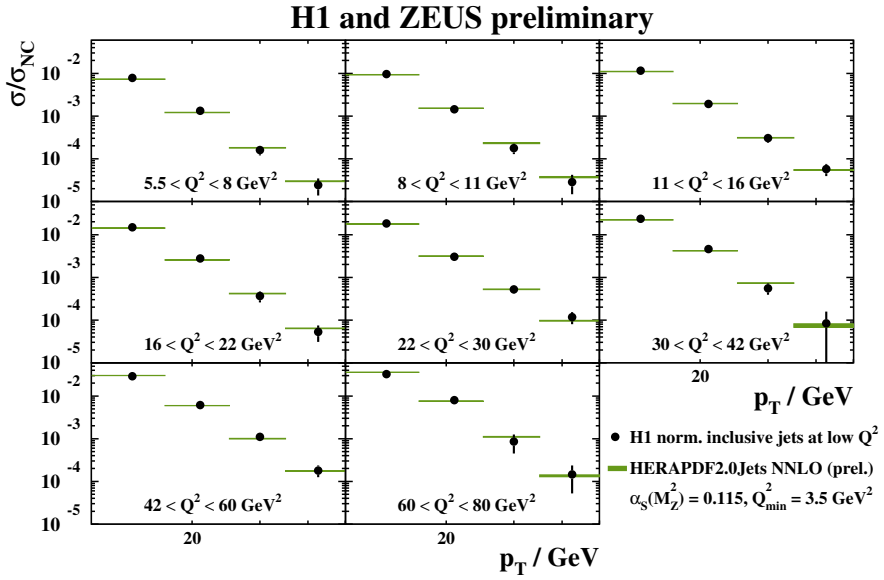

b)

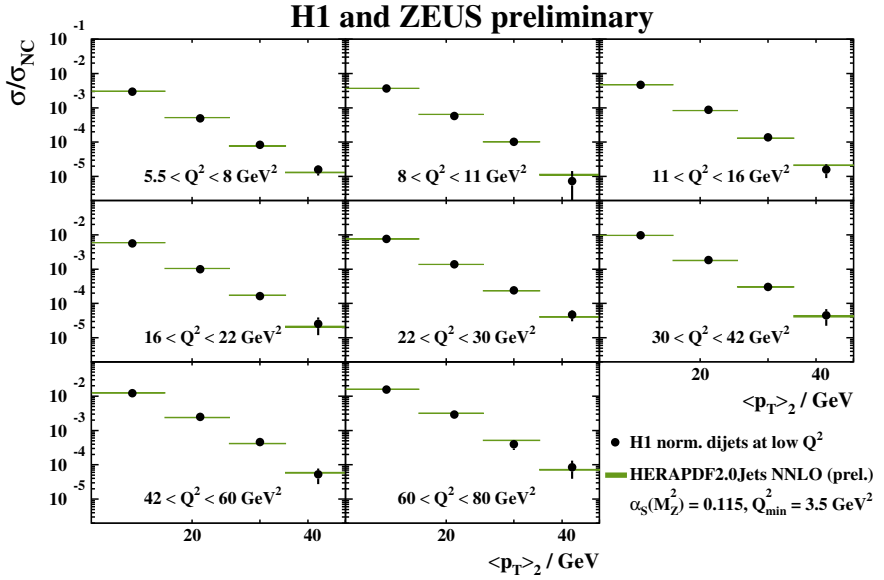

Figure 9: Differential normalised a) inclusive jet cross sections, $\mathrm{d}\sigma/\mathrm{d}p_T$, b) differential dijet cross-sections, $\mathrm{d}\sigma/\mathrm{d}\langle p_T\rangle_2$, in bins of Q^2 between 5 and 80 GeV^2 as measured by H1. The variable $\langle p_T\rangle_2$ denote the average p_T of the two jets. All cross sections are normalised to NC inclusive cross sections. Also shown are predictions from HERAPDF2.0Jets NNLO (prel.). The bands represent the total uncertainties on the predictions excluding scale uncertainties; they are mostly invisible. Only data used in the fit are shown.

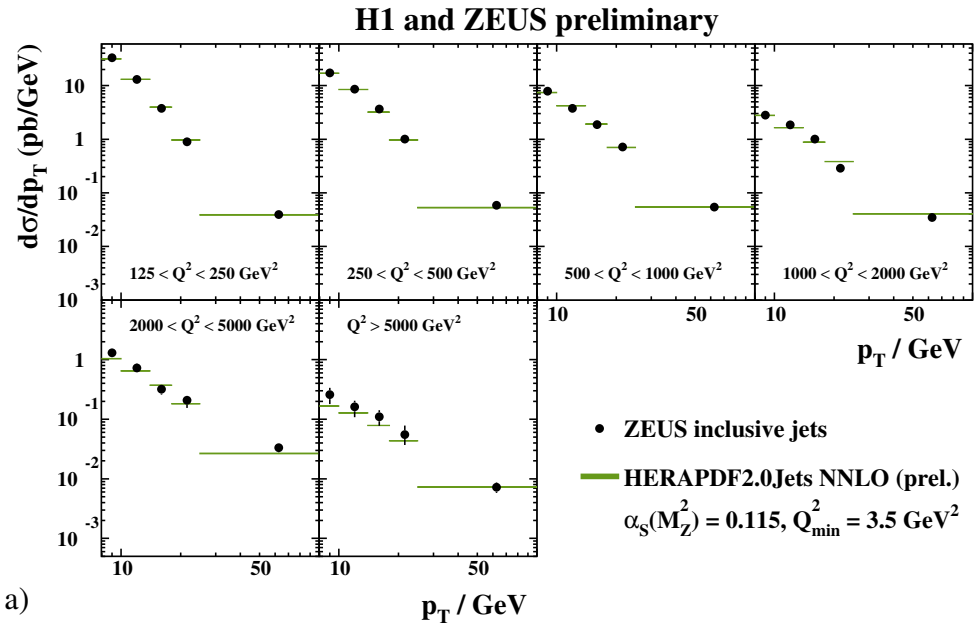

a)

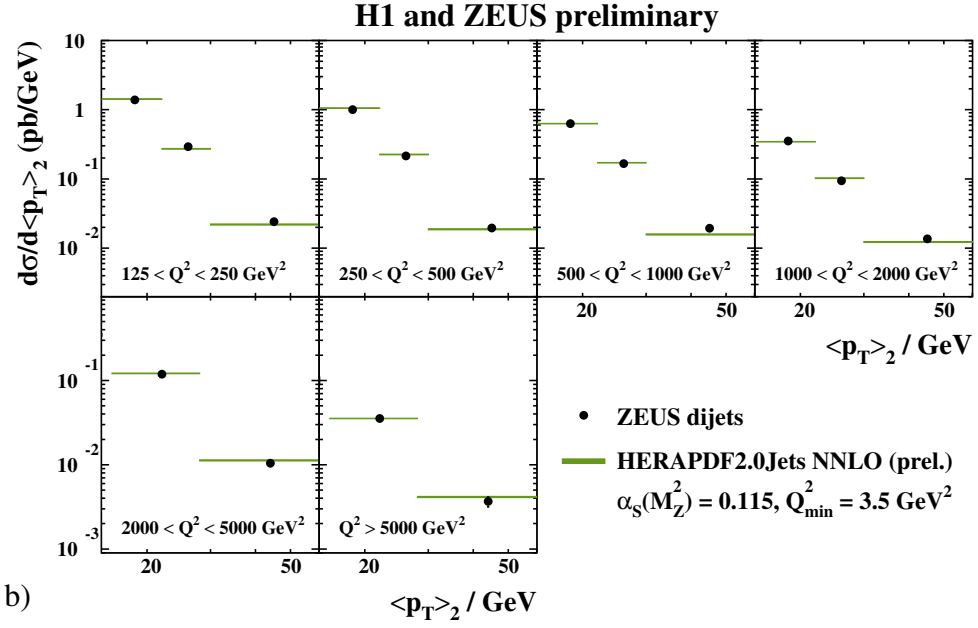

b)

Figure 10: a) Differential jet cross sections, $d\sigma/dp_T$, in bins of Q^2 between 125 and 10000 GeV^2 as measured by ZEUS. b) Differential dijet cross sections, $d\sigma/d\langle p_T\rangle_2$, in bins of Q^2 between 125 and 20000 GeV^2 as measured by ZEUS. The variable $\langle p_T\rangle_2$ denotes the average p_T of the two jets. Also shown are predictions from HERAPDF2.0Jets NNLO (prel.). The bands represent the total uncertainty on the predictions excluding scale uncertainties; they are mostly invisible. Only data used in the fit are shown.

Additional Material:

Alpha Scan plotted with experimental/fit uncertainties only:

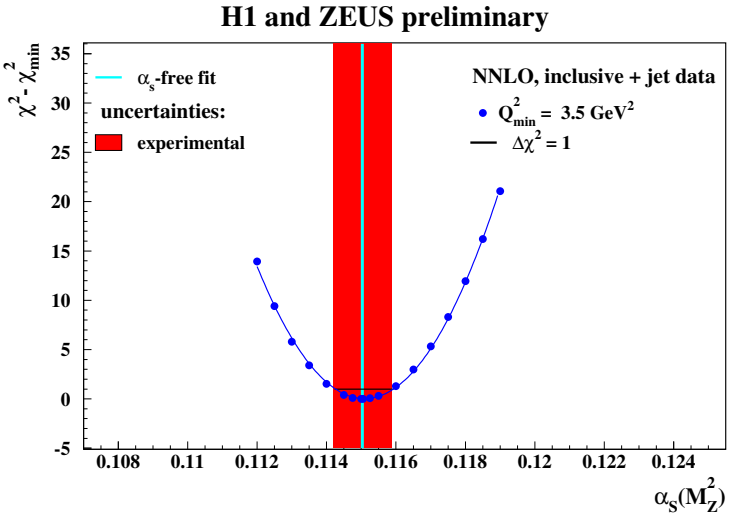

Figure 11: $\Delta\chi^2 = \chi^2 - \chi^2_{\text{min}}$ vs. $\alpha_s(M_Z^2)$ for HERAPDF2.0Jets NNLO (prel.) fits with fixed $\alpha_s(M_Z^2)$ with the standard Q^2_{min} of 3.5 GeV^2. The result and the experimental/fit uncertainty determined for the HERAPDF2.0Jets NNLO (prel.) fit with free $\alpha_s(M_Z^2)$ are also shown.

Alpha Scan plotted in old style:

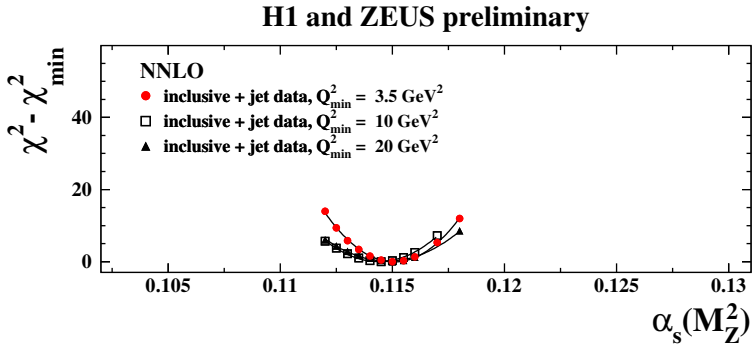

Figure 12: $\Delta\chi^2 = \chi^2 - \chi^2_{\text{min}}$ vs. $\alpha_s(M_Z^2)$ for HERAPDF2.0 NNLO (prel.) fits with fixed $\alpha_s(M_Z^2)$ with Q^2_{min} set to 3.5 GeV^2, 10 GeV^2 and 20 GeV^2 for the inclusive data.